Inorg. Chem. **2004**, *43*, 7463–7473

Binding of the Oxo–Rhenium(V) Core to Methionine and to N-Terminal Histidine Dipeptides

Christian Tessier,[†] Fernande D. Rochon,[‡] and André L. Beauchamp*[,†]

Département de Chimie, Université de Montréal, C. P. 6128, Succ. Centre-ville, Montréal, Québec, Canada H3C 3J7, and Département de Chimie, Université du Québec à Montréal, C.P. 8888, Succ. Centre-ville, Montréal, Québec, Canada H3C 3P8

Received September 1, 2004

The $ReOX_2$(met) compounds (X = Cl, Br) adopt a distorted octahedral structure in which a carboxylato oxygen lies *trans* to the Re═O bond, whereas the equatorial plane is occupied by two *cis* halides, an NH_2, and an SCH_3 group. Coordination of the SCH_3 unit creates an asymmetric center, leading to two diastereoisomers. X-ray diffraction studies reveal that the crystals of $ReOBr_2$(D,L-met)·1/2H_2O and $ReOBr_2$(D,L-met)·1/2CH_3OH contain only the *syn* isomer (S–CH_3 bond on the side of the Re═O bond), whereas $ReOCl_2$(D-met) and $ReOCl_2$(D,L-met) consist of the pure *anti* isomer. ^{1}H NMR spectroscopy shows that both isomers coexist in equilibrium in acetone (*anti*/*syn* ratio = 1:1 for X = Br, 3:1 for X = Cl). Exchange between these two isomers is fast above room temperature, but it slows down below 0 °C, and the sharp second-order spectra of both isomers at –20 °C were fully assigned. The coupling constants are consistent with the solid-state conformations being retained in solution. Complexes of the type [$ReOX_2$(His-aa)]X (X = Cl, Br) are isolated with the dipeptides His-aa (aa = Gly, Ala, Leu, and Phe). X-ray diffraction work on [$ReOBr_2$(His-Ala)]Br reveals the presence of distorted octahedral cations containing the Re═O^{3+} core and a dipeptide coordinated through the histidine residue via the imidazole nitrogen, the terminal amino group, and the amide oxygen, the site *trans* to the Re═O bond being occupied by the oxygen. The alanine residue is ended by a protonated carboxylic group that does not participate in the coordination. The constant pattern of the^{1}H NMR signals for the protons in the histidine residue confirms that the various dipeptides adopt a similar binding mode, consistent with the solid-state structure being retained in CD_3OD solution.

Introduction

Technetium and rhenium play a major role in nuclear medicine. While the γ-emitting ^{99m}Tc isotope is involved in the majority of the nuclear diagnostic scans run in hospitals,[1] the radioisotopes ^{186,188}Re are gaining considerable interest. The radiopharmaceuticals ^{186}Re-HEDP (bone palliation),[2] ^{188}Re(V)-DMSA (radiotherapeutic or prostatic treatment), and ^{188}Re-RC-160 (breast cancer)[3] have been approved or are being tested clinically. These Re isotopes present valuable characteristics, since they emit both γ and sufficiently energetic β radiations, enabling their simultaneous use for nuclear imaging and treatment.

For the past few years, our laboratories have been involved in the development of new Re(V) and Tc(V) complexes with amino acids and small peptides. These ligands are most promising as bifunctional coupling agents (BFCA) to link the radionucleus with a biologically active molecule (BAM),[4] which is either a small peptide acting as a receptor agonist or antagonist, or a monoclonal antibody.[1] Among the advantages of using amino acids or small peptides as BFCAs, let us mention their easy attachment to the BAM by derivatization or solid-phase synthesis and the tunability of the metal chelate hydrophilicity by changing the peptide side chains.[4] Various BAMs have been labeled with ^{99m}Tc complexes by the "bifunctional" method: neurotensin analogues of NT8-13 labeled with the $Tc(CO)_3^+$ core bound to N-terminal histidine,[5,6] the FDA-approved thrombus imaging agent ^{99m}Tc-P280 (where P-280 is a small oligopeptide

* Corresponding author. E-mail: andre.beauchmp@umontreal.ca. Phone: (514) 343-6446. Fax: (514) 343-7586.
[†] Université de Montréal.
[‡] Université du Québec à Montréal.

(1) Dilworth, J. R.; Parrott, S. J. *Chem. Soc. Rev.* **1998**, *27*, 43−55.
(2) Heeg, M. J.; Jurisson, S. S. *Acc. Chem. Res.* **1999**, *32*, 1053−1060.
(3) Knapp, F. F.; Beets, A. L.; Guhlke, S.; Zamora, P. O.; Bender, H.; Palmedo, H.; Biersack, H. J. *Anticancer Res.* **1997**, *17*, 1783−1795.
(4) Liu, S.; Edwards, D. S. *Chem. Rev.* **1999**, *99*, 2235−2268.
(5) Alberto, R.; Schibli, R.; Waibel, R.; Abram, U.; Schubiger, A. P. *Coord. Chem. Rev.* **1999**, *192*, 901−919.

10.1021/ic048776e CCC: $27.50
Published on Web 10/21/2004

labeled with the S-protected Cys-Gly-Cys tripeptide),[7] ^{99m}Tc-P483 (Cys-Gly-Cys), which can be used to visualize infection sites,[8] and ^{99m}Tc-P587 (Gly-Gly-Cys) and ^{99m}Tc-P829 ((β-Dap)-Lys-Cys),[9] which bind to the somatostatin receptor. Amino acids and peptides are also useful ligands as part of other strategies: the most widely used renal imaging agent is the Tc-essential complex of the $^{99m}TcO^{3+}$ core with mercaptoacetyltriglycine,[10] whereas direct ^{188}Re labeling with either octreotide or RC-160, analogues of the tetradecapeptide somatostatin, shows promises for breast cancer therapy.[1,3]

Most of the peptides used in these systems contain a thiolate donor group.[4] We are considering non-thiol-containing amino acids or small peptides as potential BFCAs, since they avoid the thiol protection step that reduces labeling efficiency and the specific activity of the labeled biomolecule. The literature on Re(V) complexes with amino acids other than the thiolate-containing cysteine or penicillamine is limited to the complex with the N_4 donor system Gly-Ala-Gly-Gly,[11] ionic compounds of the type $[ReO(dien\text{-}H)(aa)]^+$, where dien-H is deprotonated diethylenetriamine and aa is glycine, alanine, valine, leucine, or proline,[12] the $ReOX_2$(his) complexes (X = Cl, Br) containing N,N,O-tridentate histidine prepared by our research groups,[13] and the recently reported species with the tetradentate N_3O ligand 3-hydroxy-4-[2-(2′-pyridinecarboxamido)acetylamino]benzoic acid.[14]

In the first part of the present study, we are using methionine to introduce sulfur in the coordination sphere of a $ReOX_2$ core as a protected thioether group. A variety of complexes are known with ligands containing two or more thioether groups. Pietzch and co-workers recently investigated the reactivity of the $Tc(CO)_3$ and $Re(CO)_3$ moieties with a series of $RS-CH_2CH_2-SR'$ ligands, and their use as BFCAs was proposed.[15] Coordination was also found to take place with dithioether units linked to steroids[16,17] acting as anchor groups for breast tumor imaging or to functionalized tropanol moieties for labeling the dopamine transporter.[18] Thiacrown-ether complexes are known for both Tc and Re in various oxidation states,[19−23] whereas oxo−Re(V) complexes with S,S,O$^-$- or S,O$^-$,S-coordinated dithia-alcohols or bidentate $RS-CH_2CH_2-SR$ ligands have been prepared.[24−27] Tc(V)/Re(V)−monothioether compounds are less common. Complexes with various multidentate ligands containing a single central or terminal thioether group have been described,[28−35] but with methionine, the only known Tc/Re complex is $Re(CO)_3Br$(met).[36]

We are reporting here the preparation and structural characterization of $ReOX_2$(met) compounds in the solid state and in solution. These compounds were found to present the disadvantage that the prochiral SCH_3 group leads to two diastereoisomeric forms of the complexes. For this reason, we returned to the histidine residue used in our previous study and decided to introduce it into the coordination sphere as part of a dipeptide. In the second part of this work, we are showing that complexes containing the $ReOX_2$ core can be prepared with the series of N-terminal histidine dipeptides shown in Scheme 1.

Experimental Section

Reactants and Methods. K[ReO_4] (Aldrich), D- and D,L-methionine (Aldrich), the dipeptides (Sigma-Aldrich), the solvents, and all other chemicals were used as received. Deuterated solvents were purchased from CDN Isotopes. $ReOX_3(OPPh_3)(Me_2S)$ (X = Cl, Br) were prepared following the procedure of Grove and Wilkinson.[37,38]

(6) Garcia-Garayoa, E.; Allemann-Tannahill, L.; Blauenstein, P.; Willmann, M.; Carrel-Remy, N.; Tourwe, D.; Iterbeke, K.; Conrath, P.; Schubiger, P. A. *Nucl. Med. Biol.* **2001**, *28*, 75−84.
(7) Listerjames, J.; Knight, L. C.; Maurer, A. H.; Bush, L. R.; Moyer, B. R.; Dean, R. T. *J. Nucl. Med.* **1996**, *37*, 775−781.
(8) Solomon, H. F.; Derian, C. K.; Beblavy, M.; Jester, D.; Santull, R.; Pike, M.; Kroon, D.; Hoey, K.; Fischman, A. J. *J. Nucl. Med.* **1994**, *35*, 45P (abstract 172).
(9) Vallabhajosula, S.; Moyer, B. R.; Listerjames, J.; McBride, B. J.; Lipszyc, H.; Lee, H.; Bastidas, D.; Dean, R. T. *J. Nucl. Med.* **1996**, *37*, 1016−1022.
(10) Fritzberg, A. R.; Kasina, S.; Eshima, D.; Johnson, D. L. *J. Nucl. Med.* **1986**, *27*, 111−116.
(11) Benhaim, S.; Kahn, D.; Weiner, G. J.; Madsen, M. T.; Waxman, A. D.; Williams, C. M.; Clarkepearson, D. L.; Coleman, R. E.; Maguire, R. T. *Nucl. Med. Biol.* **1994**, *21*, 131−142.
(12) Melian, C.; Kremer, C.; Suescun, L.; Mombru, A.; Mariezcurrena, R.; Kremer, E. *Inorg. Chim. Acta* **2000**, *306*, 70−77.
(13) Tessier, C.; Rochon, F. D.; Beauchamp, A. L. *Inorg. Chem.* **2002**, *41*, 6527−6536.
(14) Papachristou, M.; Pirmettis, I.; Siatra-Papastaikoudi, T.; Pelecanou, M.; Tsoukalas, C.; Raptopoulou, C. P.; Terzis, A.; Chiotellis, E.; Papadopoulos, M. *Eur. J. Inorg. Chem.* **2003**, *20*, 3826−3830.
(15) Pietzsch, H. J.; Gupta, A.; Reisgys, M.; Drews, A.; Seifert, S.; Syhre, R.; Spies, H.; Alberto, R.; Abram, U.; Schubiger, P. A.; Johannsen, B. *Bioconjugate Chem.* **2000**, *11*, 414−424.
(16) Wust, F.; Skaddan, M. B.; Leibnitz, P.; Spies, H.; Katzenellenbogen, J. A.; Johannsen, B. *Bioorg. Med. Chem.* **1999**, *7*, 1827−1835.
(17) Wust, F.; Carlson, K. E.; Katzenellenbogen, J. A.; Spies, H.; Johannsen, B. *Steroids* **1998**, *63*, 665−671.
(18) Hoepping, A.; Reisgys, M.; Brust, P.; Seifert, S.; Spies, H.; Alberto, R.; Johannsen, B. *J. Med. Chem.* **1998**, *41*, 4429−4432.
(19) Pietzsch, H. J.; Spies, H.; Leibnitz, P.; Reck, G. *Polyhedron* **1993**, *12*, 2995−3002.
(20) Schibli, R.; Alberto, R.; Abram, U.; Abram, S.; Egli, A.; Schubiger, P. A.; Kaden, T. A. *Inorg. Chem.* **1998**, *37*, 3509−3516.
(21) Mullen, G. E. D.; Blower, P. J.; Price, D. J.; Powell, A. K.; Howard, M. J.; Went, M. J. *Inorg. Chem.* **2000**, *39*, 4093−4098.
(22) White, D. J.; Kuppers, H.-J.; Edwards, A. J.; Watkin, D. J.; Cooper, S. R. *Inorg. Chem.* **1992**, *31*, 5351−5352.
(23) Kuppers, H.-J.; Nuber, B.; Weiss, J.; Cooper, S. R. *J. Chem. Soc., Chem. Commun.* **1990**, 979−980.
(24) Pietzsch, H. J.; Reisgys, M.; Spies, H.; Leibnitz, P.; Johannsen, B. *Chem. Ber.* **1997**, *130*, 357−361.
(25) Reisgys, M.; Spies, H.; Johannsen, B.; Leibnitz, P.; Pietzsch, H. J. *Chem. Ber.* **1997**, *130*, 1343−1347.
(26) Pietzsch, H. J.; Spies, H.; Leibnitz, P.; Reck, G.; Johannsen, B. *Radiochim. Acta* **1993**, *63*, 163−166.
(27) Pietzsch, H. J.; Spies, H.; Leibnitz, P.; Reck, G. *Polyhedron* **1995**, *14*, 1849−1853.
(28) Glaser, M.; Howard, M. J.; Howland, K.; Powell, A. K.; Rae, M. T.; Wocadlo, S.; Williamson, R. A.; Blower, P. J. *J. Chem. Soc., Dalton Trans.* **1998**, 3087−3092.
(29) Archer, C. M.; Dilworth, J. R.; Griffiths, D. V.; Al-Jeboori, M. J.; Kelly, J. D.; Lu, C.; Rosser, M. J.; Zheng, Y. *J. Chem. Soc., Dalton Trans.* **1997**, 1403−1410.
(30) Santimaria, M.; Maina, T.; Mazzi, U.; Nicolini, M. *Inorg. Chim. Acta* **1995**, *240*, 291−297.
(31) McBride, B. J.; Baldwin, R. M.; Kerr, J. M.; Wu, J.-L.; Schultze, L. M.; Salazar, N. E.; Chinitz, J. M.; Byrne, E. F. *J. Med. Chem.* **1993**, *36*, 81−86.
(32) Fourteau, L.; Benoist, E.; Dartiguenave, M. *Synlett* **2001**, *1*, 126−128.
(33) Al-Jeboori, M. J.; Dilworth, J. R.; Hiller, W. *Inorg. Chim. Acta* **1999**, *285*, 76−80.
(34) Femia, F. J.; Babich, J. W.; Zubieta, J. *Inorg. Chim. Acta* **2000**, *300*, 462−470.
(35) Shan, X.; Espenson, J. H. *Organometallics* **2003**, *22*, 1250−1254.
(36) Kovalev, Y. G.; Ioganson, A. A. *Zh. Obsh. Khim.* **1987**, *57*, 1939−1943.
(37) Grove, D. E.; Wilkinson, G. *J. Chem. Soc. A* **1966**, 1224−1230.

Scheme 1

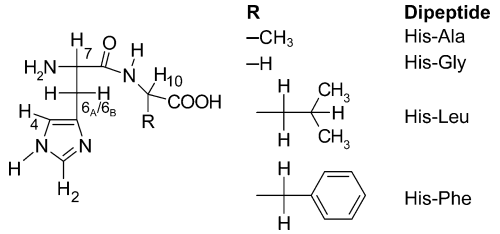

^{1}H NMR spectra were recorded on Bruker ARX-400 or DMX-600 spectrometers in deuterated methanol or acetone. The solvent signals (δ 2.05 ppm for $(CD_3)_2CO$; 3.31 ppm for CD_3OD) were used as internal references. IR spectra were recorded as KBr pellets from 4000 to 450 cm^{-1} on Perkin-Elmer 1750 FTIR or Perkin-Elmer Spectrum One spectrometers. Elemental analyses were performed at the Laboratoire d'Analyse Elémentaire de l'Université de Montréal. Mass spectra were recorded in the FAB$^+$ mode as nitrobenzylic alcohol solutions at the Centre Régional de Spectrométrie de Masse de l'Université de Montréal.

Preparative work. $ReOCl_2$(D,L-met-S,N,O)·1/2CH_3OH (1). $ReOCl_3(OPPh_3)(Me_2S)$ (0.1 mmol) is suspended in acetonitrile (15 mL), D,L-methionine (15.8 mg, 0.1 mmol) is added, and the green suspension is refluxed for 3 h. The light blue solution is filtered and evaporated to dryness. The oily residue is dissolved in a minimum of acetonitrile and precipitated with benzene. The solid is then dissolved in methanol and left overnight in the refrigerator. Dark-blue crystals of **1** are obtained. Yield: 22%. Anal. Calcd for $ReCl_2O_3NSC_5H_{10}$·1/2CH_3OH: C 15.11, H 2.77, N 3.20. Found: C 14.90, H 2.62, N 3.19. IR (KBr, cm^{-1}): 995 vs ν(Re═O). FAB$^+$-MS: m/z = 422 (M + H$^+$).

$ReOCl_2$(D-met-S,N,O) (2). Same procedure as above, from D-methionine. The product is not soluble in methanol and is simply washed with methanol. Yield: 46%. Anal. Calcd for $ReCl_2O_3NSC_5H_{10}$: C 14.25, H 2.39, N 3.32. Found: C 14.17, H 2.34, N 3.17. IR (KBr, cm^{-1}): 996 vs ν(Re═O). FAB$^+$-MS: m/z = 422 (M + H$^+$).

$ReOBr_2$(D,L-met-S,N,O)·1/2CH_3OH (3). The above procedure is applied starting with $ReOBr_3(OPPh_3)(Me_2S)$. Dark blue-green crystals are obtained. Yield: 42%. Anal. Calcd for $ReBr_2O_3NSC_5H_{10}$·1/2CH_3OH: C 12.55, H 2.30, N 2.66. Found: C 12.36, H 2.17, N 2.64. IR (KBr, cm^{-1}): 993 vs ν(Re═O). FAB$^+$-MS: m/z = 512 (M + H$^+$).

Dipeptide Complexes. $ReOX_3(OPPh_3)(Me_2S)$ (0.1 mmol) is suspended in acetonitrile (15 mL), the dipeptide (0.1 mmol) is added, and the green suspension is refluxed for 3 h. The light blue (chloro) or light green (bromo) solution is filtered off and evaporated to dryness. The oily residue is dissolved in a minimum of acetonitrile and precipitated with benzene. The solid is washed with benzene and dried in vacuo.

The bromo compounds crystallize as the pure bromide salts, but for the chloro compounds, the counterion consists of varying proportions of Cl$^-$ and [ReO_4]$^-$ ions, the latter resulting from air oxidation of Re(V) species. Mixed halide/perrhenate counterions are commonly found for oxo−rhenium complexes with nitrogen ligands.[12,39−41] Some of the solids retain lattice benzene and acetonitrile, which are not removed by extensive pumping in vacuo.

[$ReOCl_2$(His-Ala)]$Cl_{0.5}(ReO_4)_{0.5}$ (4). Yield: 42%. Anal. Calcd for $Re_{1.5}Cl_{2.5}O_6N_4C_9H_{14}$·1/2$C_6H_6$: C 21.16, H 2.52, N 8.22. Found: C 21.54, H 2.57, N 8.46. IR (KBr, cm^{-1}): 999 vs, 1017 vs ν(Re═O). FAB$^+$-MS: m/z = 499 (M$^+$).

[$ReOBr_2$(His-Ala)]Br (5). Yield: 68%. Anal. Calcd for $ReBr_3O_4N_4C_9H_{14}$·1/3C_6H_6: C 19.03, H 2.32, N 8.07. Found: C 19.31, H 2.34, N 8.17. IR (KBr, cm^{-1}): 1000 vs, 1014 vs ν(Re═O). FAB$^+$-MS: m/z = 589 (M$^+$).

[$ReOCl_2$(His-Gly)]$Cl_{0.5}(ReO_4)_{0.5}$ (6). Yield: 51%. Anal. Calcd for $Re_{1.5}Cl_{2.5}O_6N_4C_8H_{12}$·1/6$C_6H_6$: C 16.86, H 2.04, N 8.74. Found: C 16.46, H 2.03, N 8.75. IR (KBr, cm^{-1}): 1012 vs ν(Re═O). FAB$^+$-MS: m/z = 485 (M$^+$).

[$ReOBr_2$(His-Gly)]Br (7). Yield: 49%. Anal. Calcd for $ReBr_3O_4N_4C_8H_{12}$·2/5C_6H_6: C 18.23, H 2.12, N 8.17. Found: C 18.26, H 2.07, N 8.36. IR (KBr, cm^{-1}): 1010 vs ν(Re═O). FAB$^+$-MS: m/z = 575 (M$^+$).

[$ReOCl_2$(His-Phe)]$Cl_{0.9}(ReO_4)_{0.1}$ (8). Yield: 60%. Anal. Calcd for $Re_{1.1}Cl_{2.9}O_{4.4}N_4C_{15}H_{18}$·1/4$C_6H_6$: C 30.40, H 3.02, N 8.59. Found: C 30.28, H 3.12, N 8.57. IR (KBr, cm^{-1}): 1015 vs ν(Re═O). FAB$^+$-MS: m/z = 575 (M$^+$).

[$ReOBr_2$(His-Phe)]Br (9). Yield: 59%. Anal. Calcd for $ReBr_3O_4N_4C_{15}H_{18}$·5/12C_6H_6·1/4CH_3CN: C 27.47, H 2.72, N 7.56. Found: C 27.45, H 2.77, N 7.63. IR (KBr, cm^{-1}): 1015 vs ν(Re═O). FAB$^+$-MS: m/z = 665 (M$^+$).

[$ReOCl_2$(His-Leu)]$Cl_{0.7}(ReO_4)_{0.3}$ (10). Yield: 48%. Anal. Calcd for $Re_{1.3}Cl_{2.7}O_{5.2}N_4C_{12}H_{20}$·1/2$C_6H_6$: C 26.48, H 3.41, N 8.23. Found: C 26.53, H 3.24, N 8.24. IR (KBr, cm^{-1}): 1003 vs, 1014 vs ν(Re═O). FAB$^+$-MS: m/z = 541 (M$^+$).

[$ReOBr_2$(His-Leu)]Br (11). Yield: 43%. Anal. Calcd for $ReBr_3O_4N_4C_{12}H_{20}$·1/2C_6H_6·1/4CH_3CN: C 24.51, H 3.15, N 7.84. Found: C 24.14, H 3.32, N 7.90. IR (KBr, cm^{-1}): 1002 vs ν(Re═O). FAB$^+$-MS: m/z = 631(M$^+$).

Crystallographic Measurements and Structure Determination. Blue crystals of $ReOCl_2$(D-met) (**2**) and $ReOBr_2$(D,L-met)·1/2H_2O (**3a**) were obtained by recrystallization in acetonitrile. Crystals of solvent-free $ReOCl_2$(D,L-met) (**1a**) formed upon cooling of the acetonitrile reaction mixture. Those of $ReOBr_2$(D,L-met)·1/2CH_3OH (**3**) precipitated from a methanol solution left overnight in the refrigerator. The X-ray data on **1a**, **3**, and **3a** were collected at room temperature with an Enraf-Nonius CAD-4 diffractometer using graphite-monochromatized Cu Kα radiation under the control of the CAD-4 software.[42] The data set for **2** was obtained from a Bruker P-4 diffractometer under the control of the XSCANS software,[43] using graphite-monochromatized Mo Kα radiation. All calculations were carried out with the SHELXTL system.[44] The XPREP procedure[45] was used to apply an absorption correction based on crystal morphology and to determine the Laue symmetry, systematic absences, and space group. The structures were solved by direct methods or the heavy-atom method with SHELXS.[46] The heavy atoms were initially found, and the remaining atoms were then located from structure-factor calculations and ΔF maps with SHELXL.[47] The structure was refined by least squares on F^2. The

(38) Bryan, J. C.; Stenkamp, R. E.; Tulip, T. H.; Mayer, J. M. *Inorg. Chem.* **1987**, *26*, 2283−2288.
(39) Lebuis, A. M.; Young, J. M. C.; Beauchamp, A. L. *Can. J. Chem.* **1993**, *71*, 2070−2078.
(40) Bélanger, S.; Beauchamp, A. L. *Inorg. Chem.* **1996**, *35*, 7836−7844.
(41) Bélanger, S.; Fortin, S.; Beauchamp, A. L. *Can. J. Chem.* **1997**, *75*, 37−45.
(42) *CAD-4 Software, version 5.0*; Enraf-Nonius: Delft, The Netherlands, 1989.
(43) *XSCANS, X-ray Single-Crystal ANalysis Software, PC Version 5*; Bruker AXS Inc.: Madison, WI, 1995.
(44) *SHELXTL, The Complete Software Package for Single-Crystal Structure Determination, Release 5.10*; Bruker AXS Inc.: Madison, WI, 1997.
(45) *XPREP, X-ray Data Preparation and Reciprocal Space Exploration Program, Release 5.10*; Bruker AXS Inc.: Madison, WI, 1997.
(46) Sheldrick, G. M. *SHELXS-97, Program for the Solution of Crystal Structures*; University of Göttingen: Göttingen, Germany, 1997.
(47) Sheldrick, G. M. *SHELXL-96, Program for the Refinement of Crystal Structures*; University of Göttingen: Göttingen, Germany, 1996.

Table 1. Crystal Data

	1a	2	3	3a	5a
name	$ReOCl_2$(D,L-met)	$ReOCl_2$(D-met)	$ReOBr_2$(D,L-met)·1/2CH_3OH	$ReOBr_2$(D,L-met)·1/2H_2O	[$ReOBr_2$(His-Ala)]-Br·1/2H_2O·2CH_3CN
chemical formula	$C_5H_{10}Cl_2NO_3ReS$	$C_5H_{10}Cl_2NO_3ReS$	$C_{5.5}H_{12}Br_2NO_{3.5}ReS$	$C_5H_{11}Br_2NO_{3.5}ReS$	$C_{13}H_{21}Br_3N_6O_{4.5}Re$
M_w	421.30	421.30	526.24	519.23	759.32
space group	$P2_1/c$ (No. 14)	$P2_12_12_1$ (No. 19)	$P2_1/c$ (No. 14)	$P2_1/c$ (No. 14)	$P2_12_12_1$ (No. 19)
a (Å)	7.665(2)	5.976(1)	10.650(3)	10.500(3)	11.0459(3)
b (Å)	10.834(3)	7.127(1)	15.659(4)	15.629(6)	18.7300(6)
c (Å)	38.87(2)	25.232(7)	15.021(5)	14.669(5)	22.9226(7)
β (deg)	94.77(3)		100.28(2)	98.94(3)	
V (Å^3)	3217(2)	1074.7(4)	2465(1)	2378(1)	4742.4(2)
Z	12	4	8	8	8
ρ_{calcd} (g cm^{-3})	2.610	2.604	2.836	2.901	2.127
μ (mm^{-1})	28.42	11.97	16.50	29.42	16.23
λ (Å)	1.54178	0.71073	0.71073	1.54178	1.54178
cryst size (mm^3)	0.50 × 0.20 × 0.06	0.60 × 0.17 × 0.06	0.16 × 0.08 × 0.04	0.48 × 0.11 × 0.08	0.52 × 0.09 × 0.06
measured reflns	23295	12422	18962	14695	29103
indep reflns (R_{int})	6103 (0.057)	3129 (0.058)	4837 (0.094)	4494 (0.099)	8679 (0.0046)
obsd reflns ($I > 2\sigma(I)$)	5747	3022	3308	3891	5202
ranges of h, k, l	$-9 \le h \le 9$ $-13 \le k \le 13$ $-47 \le l \le 47$	$-8 \le h \le 8$ $-10 \le k \le 10$ $-35 \le l \le 35$	$-13 \le h \le 13$ $-19 \le k \le 19$ $-18 \le l \le 18$	$-12 \le h \le 12$ $-19 \le k \le 19$ $-17 \le l \le 17$	$-10 \le h \le 12$ $-22 \le k \le 22$ $-27 \le l \le 23$
R_1[a] ($I > 2\sigma(I)$)	0.0364	0.0270	0.0562	0.0485	0.0541
wR_2	0.0868	0.0710	0.1262	0.1498	0.0860
S	1.275	1.201	1.020	1.049	0.877
Flack[84]		0.005(11)			0.033(11)

[a] $R_1 = \sum(||F_o| - |F_c||)/\sum|F_o|$, $wR_2 = [\sum(w(F_o^2 - F_c^2)^2)/\sum(w(F_o^2)^2)]^{1/2}$, $S = [\sum[w(F_o^2 - F_c^2)^2]/(N_{reflns} - N_{params})]^{1/2}$.

non-hydrogen atoms were generally refined anisotropically. The hydrogens were first placed at idealized positions with the standard (C,N,O)−H distances of SHELXL and allowed to ride on the supporting atom. Their isotropic temperature factors U_{iso} were fixed at values related to the equivalent temperature factor U_{eq} of the supporting atom by $U_{iso} = k \times U_{eq}$ (where $k = 1.5$ (methyl, hydroxyl) or 1.2 (others)). ORTEP diagrams were produced with the XP routine of SHELXTL. Crystal data are given in Table 1.

Blue needles of [$ReOBr_2$(His-Ala)]Br·1/2H_2O·2CH_3CN (**5a**) were obtained by recrystallization in acetonitrile. A crystal was mounted on a Bruker SMART CCD 2K diffractometer operating with graphite-monochromatized Cu Kα radiation and controlled by the SMART software.[48] The intensity data were collected over a period of 16 h at room temperature, and they showed a decay of 14.7%. The SAINT program[49] was used for cell refinement and data reduction, whereas an empirical absorption correction was applied using SADABS.[50] The asymmetric unit contained two independent molecules. The coordinates of the Re atoms were determined by direct methods,[46] and the positions of all other non-hydrogen atoms were found by the standard Fourier technique.[47] Abnormally large thermal ellipsoids indicated that the carboxylic unit was disordered in both molecules. These carboxylic groups were connected by a pair of complementary O−H···O hydrogen bonds of the type commonly found in carboxylic acids. Since these systems often show twofold orientation disorder corresponding to a 180° rotation about the C_α−CO_2 bond, idealized rigid carboxylic groups (C═O = 1.207 Å, C−OH = 1.306 Å, O···O(H) = 2.223 Å; C_α···O = 2.397 Å, C_α···O(H) = 2.352 Å) were defined, and coplanarity was imposed by the FLAT option of SHELXL. Two such units initially oriented 180° apart were defined, so that each oxygen "region" is occupied by equal amounts of carbonyl and hydroxyl oxygens. These atomic positions were refined anisotropically, while the occupancies were fixed to 0.50 and the geometrical constraints were retained. For the hydrogens of the carboxylic groups and water molecule, idealized positions were calculated by considering the positions of the hydrogen-bond acceptors (Br^- ions in the case of water). Crystal data are listed in Table 1.

Scheme 2

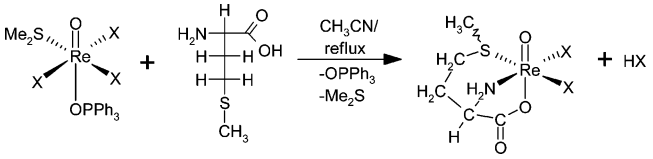

Results and Discussion

Reactions with Methionine. The $ReOX_2$(met) compounds are formed in blue (X = Cl) or blue-green solutions (X = Br) by refluxing 1 equiv of methionine with $ReOX_3(OPPh_3)(Me_2S)$ in acetonitrile (Scheme 2). The pure solids are obtained by recrystallization in methanol. Elemental analyses and mass spectra (*m*/*z* and isotopic distribution of the parent peak) are consistent with the $ReOX_2$(met) formula. Crystallographic work (see below) shows that methionine is tridentate S,N,O-coordinated. Thus, the coordination sphere is similar to that of the corresponding histidine complexes $ReOX_2$(his),[13] with replacement of the imidazole ring by the $-SCH_3$ group. However, the thioether is a prochiral group, and its coordination generates two diastereoisomers that differ by the methyl group pointing either on the same side as the Re═O bond (*syn*) or in the opposite direction (*anti*). Both isomers are formed, as evidenced from the NMR spectra and crystal structures to be discussed below.

The IR data and tentative assignments are listed in Table S-1 (Supporting Information). The strong Re═O stretching mode is found at ∼995 cm^{-1}, a relatively high wavenumber, which suggests that the Re−carboxylate bond *trans* to the

(48) *SMART, Bruker Molecular Analysis Research Tool, Release 5.059*; Bruker AXS Inc.: Madison, WI, 1999.
(49) *SAINT, Integration Software for Single Crystal Data, Release 6.06*; Bruker AXS Inc.: Madison, WI, 1999.
(50) Sheldrick, G. M. *SADABS, Bruker Area Detector Absorption Corrections*; Bruker AXS Inc.: Madison, WI, 1996.

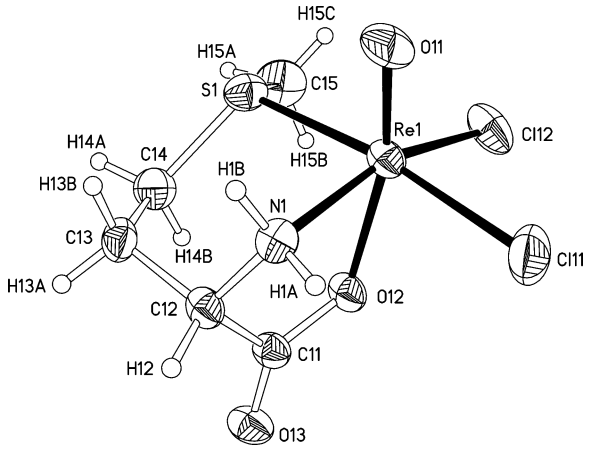

Figure 1. ORTEP drawing of one of the three independent molecules in the asymmetric unit of $ReOCl_2$(D,L-met) (**1a**). The other two molecules have a very similar structure. In the numbering scheme, the first digit corresponds to the number of the molecule, and the second digit (on H, O, and Cl) indicates the position. Ellipsoids correspond to 40% probability.

Table 2. Selected Bond Lengths (Å) in the Methionine Complexes

	Re−O1	Re−O2	Re-X1	Re-X2	Re−N	Re−S
1a	1.665(5)	2.059(4)	2.352(2)	2.334(2)	2.147(5)	2.429(2)
	1.665(4)	2.029(4)	2.377(2)	2.341(2)	2.147(5)	2.416(2)
	1.658(5)	2.088(4)	2.354(2)	2.338(2)	2.147(4)	2.400(2)
2	1.673(4)	2.049(5)	2.378(2)	2.333(2)	2.160(5)	2.421(2)
3	1.659(11)	2.052(10)	2.502(2)	2.490(2)	2.167(11)	2.431(3)
	1.643(10)	2.069(9)	2.516(2)	2.481(2)	2.162(12)	2.420(4)
3a	1.657(7)	2.068(7)	2.506(1)	2.489(1)	2.154(8)	2.432(2)
	1.667(8)	2.064(7)	2.508(1)	2.481(1)	2.137(8)	2.432(3)

oxo ligand is not very strong. Coordination of the carboxylate group is confirmed by the shift to higher energy of the $\nu_a(CO_2)$ mode (∼1620 cm^{-1}) to ∼1700 cm^{-1}, indicating that the carbonyl bond of the coordinated molecule has a high double-bond character. Other variations of the ligand vibrations upon coordination are discussed in the Supporting Information.

Crystal Structures. $ReOCl_2$(D,L-met) (1a) and $ReOCl_2$(D-met) (2). Both compounds consist of distorted octahedral molecules in which methionine is S,N,O-tridentate (Figure 1). The thioether unit, the NH_2 group, and two chlorine ligands occupy the equatorial plane, whereas a carboxylato oxygen lies *trans* to the Re═O bond in the axial direction. Compounds **1a** and **2** both contain only the *anti* isomer (S-methyl group away from the Re═O bond), where the two asymmetric centers (amino acid central carbon and coordinated S atom) exhibit the same chirality (S_SC_S or S_RC_R). Figure 1 shows one of the three crystallographically independent molecules of **1a**, which contains the L-met form and corresponds to the S_SC_S pattern. In this racemic crystal prepared from D,L-met, the unit cell inversion centers generate an equal number of S_RC_R enantiomers. Compound **2** was prepared from D-met, and it contains only the S_RC_R enantiomer.

Selected bond lengths are listed in Table 2. The Re═O (1.665−1.673 Å) and Re−NH_2 (2.147−2.160 Å) distances compare well with those found in the corresponding histidine−Re(V) complexes.[13] The Re−O(carboxylato) distances (2.029−2.088 Å) are also similar, although they exhibit a greater variability, probably because hydrogen bonding to the uncoordinated oxygen and other packing effects introduce significant changes in the orientation of the carboxylate for the different molecules. In agreement with the *trans* influence of the thioether group being greater than that of an amine, the Re−Cl1 bonds (2.352−2.378 Å), *trans* to S, are systematically longer than Re−Cl2 (2.333−2.341 Å), *trans* to N (Δ/σ ratio between 3.7 and 15). Comparisons among the structures found in the Cambridge Structural Database[51] reveal that the Re−S bond is also sensitive to the *trans* donor atom: the typical Re−S distance is 2.30 Å (σ = 0.04 Å, 176 entries) for *trans* N or O donors, while it increases to 2.42 Å (σ = 0.05 Å, 26 entries) for *trans* Cl or Br atoms. Our compounds belong to the latter type, and our Re−S bonds (2.400−2.429 Å) lie close to the expected value.

The angles listed in Table S-2 (Supporting Information) describe an octahedron showing distortions similar to those noted for complexes with other amino acids.[13,52−54] The Re atom is displaced 0.24−0.30 Å from the "equatorial" plane on the oxo side, which results in all *cis*-O═Re−L angles being generally >90°, especially those involving the Re−Cl bonds (95.9−106.5°). This also leads to large departures from 180° for the *trans* angles: N−Re−Cl2 = 162−165°; S−Re−Cl1 = 167−172°; O═Re−O = 164−167°. The carboxylato oxygen and the amino group coordinate normally, with Re−O−C1 and Re−N−C2 (mean) angles of ∼122.3° and 111.1°, respectively, but the formation of the five-membered ring reduces the N−Re−O bite angle to ∼75°. In the pyramidal environment of the S atoms, the Re−S−C angles (107.1−114.0°, mean = 109.8°) are close to the pseudotetrahedral value, but the C−S−C angles are ∼10° smaller (98.7−100.1°, mean = 99.3°).

The six-membered Re/S/C4/C3/C2/N ring exhibits an approximate chair conformation. The data in Table S-3 (Supporting Information) show that, for each of the three mean planes through opposite bonds (Re/S/C3/C2, S/C4/C2/N, and Re/N/C3/C4), the two remaining atoms show displacements of 0.59−1.20 Å on opposite sides of the plane. For a perfect chair arrangement, the six torsion angles around the ring should be equal with a sign alternance: the −49°/62°/−79°/81°/−59°/42° pattern observed (Table S-4) shows the expected alternance. Interestingly, this conformation leads to a relatively short H1B···H3B distance of 2.25 Å, which is reflected in the ^{1}H NMR data to be discussed below. The five-membered Re/N/C2/C1/O2 ring exhibits an envelope conformation, in which the Re, N, C1, and O2 atoms define an approximate plane and C2 is offset by ∼0.52 Å (Table S-3).

The molecules are held in the unit cell by an extended network of hydrogen bonds formed by the amine protons with the carboxylate oxygens and the Cl ligands (Figures S-1 and S-2). Details are provided in Table S-5. The fact that these interactions are different for the three independent molecules in compound **1** explains the small differences

(51) *Cambridge Structural Database*, 5.24 ed.; Cambridge Crystallographic Data Centre: Cambridge, England, 2002.
(52) Kirsch, S.; Noll, B.; Spies, H.; Leibnitz, P.; Scheller, D.; Krueger, T.; Johannsen, B. *J. Chem. Soc., Dalton Trans.* **1998**, 455−460.
(53) Kirsch, S.; Jankowsky, R.; Leibnitz, P.; Spies, H.; Johannsen, B. *J. Biol. Inorg. Chem.* **1999**, *4*, 48−55.
(54) Chatterjee, M.; Achari, B.; Das, S.; Banerjee, R.; Chakrabarti, C.; Dattagupta, J. K.; Banerjee, S. *Inorg. Chem.* **1998**, *37*, 5424−5430.

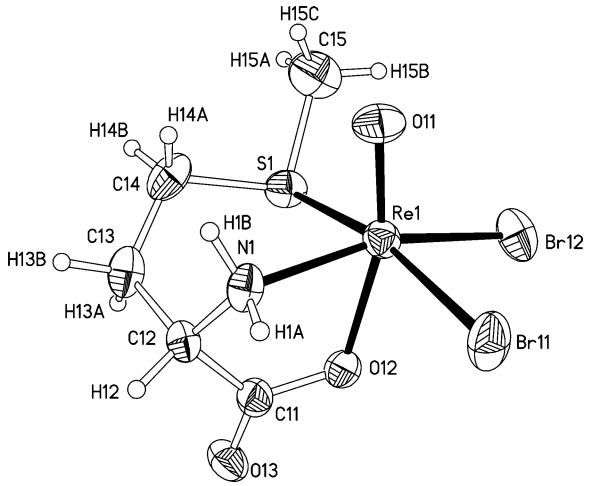

Figure 2. ORTEP drawing of one of the two independent molecules in the asymmetric unit of $ReOBr_2$(D,L-met)·1/2H_2O (**3a**). The other molecule has a very similar structure. In the numbering scheme, the first digit corresponds to the number of the molecule, and the second digit (on H, O, and Cl) indicates the position. Ellipsoids correspond to 40% probability.

observed in the bond lengths and other structural features involving the acceptor atoms.

$ReOBr_2$(D,L-met)·1/2CH_3OH (3) and $ReOBr_2$(D,L-met)·1/2H_2O (3a). These compounds are isostructural, the lattice water molecule of **3a** being replaced by methanol in **3**. The coordination sphere of rhenium (Figure 2) is the same as in the above chloro compounds, but in this case, the *syn* isomer (S−CH_3 bond on the same side as the Re═O bond) is isolated. Since the compounds are racemic, their unit cells contain an equal number of S_RC_S and S_SC_R enantiomers.

The bond lengths and angles are listed in Tables 2 and S-2, respectively. The Re−Br bonds are similar to those found for the histidine complex.[13] As noted above, the Re−Br1 bonds (mean 2.508 Å) are slightly longer than Re−Br2 (mean 2.485 Å) because of the *trans* influence of the thioether group. Replacing Cl by larger Br atoms does not greatly affect the remaining bond lengths and angles, except for a small increase of the (mean) X1−Re−X2 angle from 88.4° (Cl) to 89.7° (Br). The orientation of the S-methyl groups introduces important changes around the S atom: the C5−S−C4, C5−S−Re, and C4−S−Re angles of 99.3°, 111.8°, and 107.7° (*anti*, Cl) become 102.3°, 107.2°, and 101.2° (*syn*, Br), respectively. The S−Re−O "bite angle" in the seven-membered ring is reduced from 84.7° (Cl) to 78.9° (Br).

In this *syn* arrangement, the five-membered ring (Re, O2, C1, C2, N) exhibits a half-chair conformation. The six-membered Re/S/C4/C3/C2/N ring adopts a distorted boat conformation: the Re, S, C3, and C2 atoms are roughly coplanar (deviations 0.12−0.20 Å), whereas N and C4 are displaced by 0.71 and 0.86 Å, respectively, on the same side of the plane (Table S-3). The sequence of torsion angles (starting with Re−S−C4−C3, S−C4−C3−C2...) is −69°/52°/33°/−84°/45°/20° (Table S-4), that is, in agreement with the typical $-\tau/\tau/\tau/-\tau/\tau/\tau$ pattern for a boat conformation. It this arrangement, a relatively close contact of 2.26 Å exists between H1B and H4A. Methionine does not commonly adopt such a boat conformation: for the sample of 25 S,N,O- or S,N-coordinated methionines in the 18 transition-metal complexes found in the Cambridge Structural Database[51] (Table S-6), the *syn* configuration was observed 14 times, usually with a chair conformation. The only two examples of a boat conformation[55,56] involve tridentate methionine, and the crystals are disordered, the *syn*-boat molecules sharing a crystallographic site with more abundant *anti* molecules. It could be argued that the *syn* isomer in these crystals is forced into a boat conformation by the crystallographic framework defined mainly by the *anti* isomer, but this assumption could hardly hold in the present case, since the *syn* isomer was obtained for both of our bromo compounds, whose crystal packing is totally different. Therefore, we will assume that this is the most stable arrangement for the *syn* isomer of our $ReOX_2$(met) compounds.

The complexes are held together by a network of hydrogen bonds in which the lattice water or methanol molecules participate. Details are provided in Figure S-3 and Table S-5.

^{1}H NMR Spectroscopy of the Methionine Complexes. The crude product from acetonitrile was soluble in CD_3OD, and spectra taken in this solvent showed both broad and well-resolved signals. The latter signals were identified as those of protonated methionine ($metH_2^+$, Table 3). After recrystallization in methanol, the solids became insoluble in this solvent, and the study was pursued in deuterated acetone. The sharp peaks of protonated methionine were no longer present, but the remaining signals remained broad at room temperature, even at 600 MHz, indicating that an exchange process was underway. At 0 °C and 600 MHz, the broad signals split into two sets of sharp peaks, with an approximate intensity ratio of 3:1 for the chloro complexes (**1** and **2**) and 1:1 for the bromo complexes (**3a** and **3**). They were assigned to the *syn* and the *anti* isomers.

The spectrum of the chloro complex at −20 °C is shown in Figure 3, where the signals are assigned according to the atom labeling scheme used for the crystal structures. The spectra are rather complex, since C_2 is an asymmetric center, making the H_{3A}/H_{3B} and H_{4A}/H_{4B} protons nonequivalent. All signals in each set could be assigned from 2D spectra at −10 °C, but the spectra were second-order and simulations were required. The strategy applied is described in detail in the Supporting Information. The chemical shifts and coupling constants listed in Tables 3−5 for these protons were obtained by simulation with the NUTS software.[57]

These assignments were checked for overall consistency by comparing the torsion angles predicted from the coupling constants by the MULDER program[58] with those found in the crystal structures (Table 5). The ranges given in Table 5 are based on the assumption that the coupling constants are known to within ±0.5 Hz. The agreement between experimental and calculated torsion angles is very good, not only for the common *trans* (180°) or *gauche* (60°) interactions, but also for nonstandard relative orientations. For instance, the small couplings of 1.0−1.5 Hz observed between H_2 and

(55) Balakaeva, T. A.; Churakov, A. V.; Ezernitskaya, M. G.; Kuz'mina, L. G.; Lokshin, B. V.; Efimenko, I. A. *Russ. J. Coord. Chem.* **1999**, *25*, 579−583.
(56) Hambley, T. H. *Acta Cyrstallogr., Sect. B.* **1988**, *44*, 601−609.
(57) *NUTS*, 5.084 ed.; Acorn NMR: Livermore, CA, 1995.
(58) Padrta, P.; Sklenar, V. *J. Biomol. NMR* **2002**, *24*, 339−349.

Table 3. Chemical Shifts (ppm) of Methionine and Its Complexes

molecule	H_{1A}[c]	H_{1B}[c]	H_2	H_{3A}	H_{3B}	H_{4A}	H_{4B}	H_5
metH[a]			3.669	2.190; 2.036		2.637; 2.610		2.122
$metH_2^{+}$[a]			4.148	2.256; 2.151		2.692; 2.678		2.145
$metH_2^{+}$[b]	8.350		4.529	2.324		2.869; 2.769		2.104
anti-$ReOCl_2$(met)[b]	11.05	7.42	4.507	2.708	2.676	4.185	2.340	2.717
anti-$ReOBr_2$(met)[b]	11.03	7.54	4.405	2.732	2.748	4.086	2.448	2.808
syn-$ReOCl_2$(met)[b]	10.86	7.20	4.789	2.537	3.145	3.672	4.643	2.970
syn-$ReOBr_2$(met)[b]	10.86	7.26	4.740	2.534	3.174	3.652	4.692	2.993

[a] In CD_3OD, RT. [b] In acetone-d_6, −20 °C. [c] Variations within ±0.05 ppm were observed from one sample to another for the NH_2 signals.

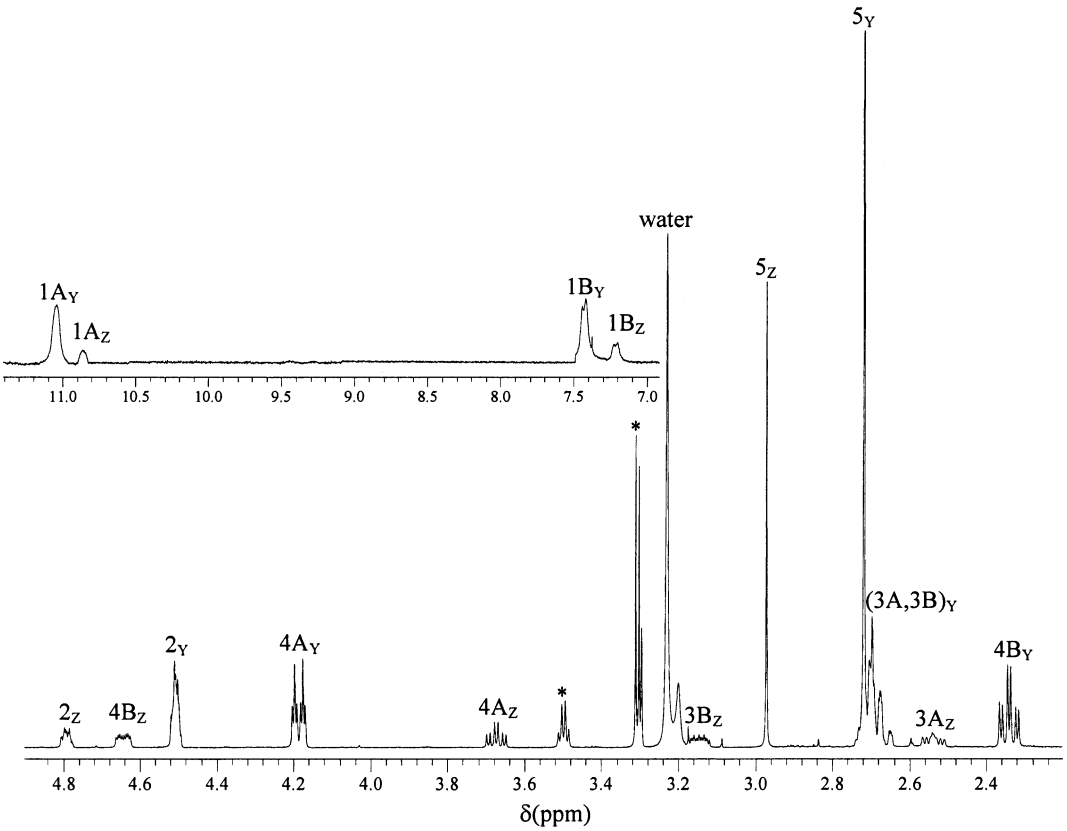

Figure 3. ^1H NMR spectrum of $ReOCl_2$(D,L-met) (**1**) in acetone at −20 °C. The signals are identified according to the proton numbering scheme used for X-ray work (Figures 1 and 2), Y = *anti* isomer, Z = *syn* isomer. Asterisks indicate traces of CH_3OH.

Table 4. Geminal Coupling Constants (Hz) of Methionine and Its Complexes

molecule	$^2J(H_{3A}-H_{3B})$	$^2J(H_{4A}-H_{4B})$
MetH[a]	14.5	13.4
$MetH_2^{+}$[a]	14.6	13.5
anti-$ReOCl_2$(met)[b]	16.1	12.8
anti-$ReOBr_2$(met)[b]	16.7	13.2
syn-$ReOCl_2$(met)[b]	15.6	12.7
syn-$ReOBr_2$(met)[b]	15.5	12.5

[a] In CD_3OD, RT. [b] In acetone-d_6, −20 °C.

H_{3B} (*anti*) and between H_2 and H_{3A} (*syn*) are in good agreement with the near orthogonality of the corresponding C−H bonds in the structure. Similarly, the values of −37° for $H_{3A}-C_3-C_2-H_2$ (*anti*) and 31° for $H_{3B}-C_3-C_2-H_2$ (*syn*) are correctly predicted from the coupling constants. The only case where the difference is appreciable is the $H_{1B}-N-C_2-H_2$ angle, but it is not totally surprising that the parameters of the MULDER software, based on free peptides and amino acids, do not reproduce perfectly the behavior of protons very close to the metal center.

The dynamics of substituent inversion has been studied for various coordinated thioethers,[59] but quantitative studies for methionine have been conducted only with Pd and Pt complexes, for which $\Delta G^{\ddagger}$ values of 50−75 kJ/mol were observed.[60−64] The parameters for the exchange between our *syn* and *anti* molecules were determined for compound **1a** from a series of spectra recorded at 400 MHz between −43 and +27 °C in acetone. Data are provided in Table S-7 (Supporting Information). Arrhenius and Eyring plots gave the following estimated thermodynamic parameters: T_c =

(59) Abel, E. W.; Bhargava, S. K.; Orrell, K. G. *Prog. Inorg. Chem.* **1984**, *32*, 1−118.
(60) Ankersmit, H. A.; Veldman, N.; Spek, A. L.; Eriksen, K.; Goubitz, K.; Vrieze, K.; Vankoten, G. *Inorg. Chim. Acta* **1996**, *252*, 203-219.
(61) Ankersmit, H. A.; Witte, P. T.; Kooijman, H.; Lakin, M. T.; Spek, A. L.; Goubitz, K.; Vrieze, K.; Vankoten, G. *Inorg. Chem.* **1996**, *35*, 6053−6063.
(62) Norman, R. E.; Ranford, J. D.; Sadler, P. J. *Inorg. Chem.* **1992**, *31*, 877−888.
(63) Galbraith, J. A.; Menzel, K. A.; Ratilla, E. M. A.; Kostic, N. M. *Inorg. Chem.* **1987**, *26*, 2073−2078.
(64) Gummin, D. D.; Ratilla, E. M. A.; Kostic, N. M. *Inorg. Chem.* **1986**, *25*, 2429−2433.

Scheme 3

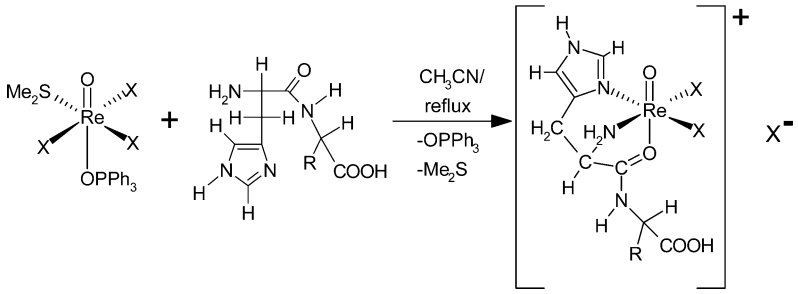

Table 5. Comparison of the Torsion Angles Derived from the Vicinal Coupling Constants with Those Determined by X-ray Diffraction for the Methionine Complexes

	$ReOCl_2$(met)[b]			$ReOBr_2$(met)[b]	
	angle (deg)[a]	^3J (Hz)	angle (deg)[c]	^3J (Hz)	angle (deg)[c]
		anti (Y)			
$H_{3A}-C_3-C_2-H_2$	−37.1	6.0	−37/−45	6.7	−32/−40
$H_{3B}-C_3-C_2-H_2$	79.0	1.4	65/97	1.6	63/100
$H_{3A}-C_3-C_4-H_{4A}$	54.3	3.7	46/54	3.8	44/52
$H_{3A}-C_3-C_4-H_{4B}$	−62.5	3.3	−58/−67	2.7	−63/−72
$H_{3B}-C_3-C_4-H_{4A}$	−61.9	3.4	−59/−67	4.1	−55/−62
$H_{3B}-C_3-C_4-H_{4B}$	176.6	14.1	170/180	13.0	171/180
$H_{1A}-N-C_2-H_2$	35.9	5.1	35/42	5.0	35/43
$H_{1B}-N-C_2-H_2$	−82.2	3.5	−56/−64	3.2	−59/−67
		syn (Z)			
$H_{3A}-C_3-C_2-H_2$	−84.2	1.1	−84/−101	1.2	−81/−103
$H_{3B}-C_3-C_2-H_2$	31.4	7.8	22/31	7.8	22/31
$H_{3A}-C_3-C_4-H_{4A}$	168.4	12.2	171/180	12.5	171/180
$H_{3A}-C_3-C_4-H_{4B}$	50.4	5.8	41/49	6.0	40/47
$H_{3B}-C_3-C_4-H_{4A}$	52.8	5.4	42/50	5.4	42/50
$H_{3B}-C_3-C_4-H_{4B}$	−65.2	3.3	−60/−68	2.7	−65/−74
$H_{1A}-N-C_2-H_2$	34.9	5.5	32/39	5.0	35/42
$H_{1B}-N-C_2-H_2$	−83.8	4.1	−52/−60	3.8	−54/−62

[a] From the crystal structure. [b] Calculated with the MULDER software.[58] [c] Range of torsion angles, assuming that the coupling constants are known to within ±0.05 Hz.

297 K, E_a = 8.0 kJ/mol, $\Delta H^{\ddagger}$ = 6.0 kJ/mol, $\Delta S^{\ddagger}$ = −182 J/(K·mol), and $\Delta G^{\ddagger}_{297}$ = 60.0 kJ/mol. The $\Delta G^{\ddagger}$ value agrees with the results obtained for Pt/Pd−methionine complexes (mean $\Delta G^{\ddagger}$ = 62 kJ/mol, σ = 7 kJ/mol, 19 data)[60−64] as well as for thioether rhenium(I) complexes ($\Delta G^{\ddagger}$ = 61 kJ/mol, σ = 10 kJ/mol, 35 data).[59]

Reactions with the Dipeptides. The blue (chloro) or blue-green (bromo) $[ReOX_2(His\text{-}aa)]^+$ cationic species are obtained from $ReOX_2(OPPh_3)(Me_2S)$ by reacting with 1 equiv of the dipeptide in acetonitrile (Scheme 3). Elemental analyses and mass spectra (*m*/*z* and isotopic distribution of the parent peak) are consistent with the $[ReOX_2(His\text{-}aa)]X$ formula. For the chloro complexes, elemental analysis shows that the Cl^- counterion is replaced by ReO_4^- (produced by air oxidation) in various proportions not exceeding 50%, as sometimes noted for oxo−rhenium complexes prepared from halogen containing precursors.[12,39−41] Crystallographic work (see below) shows that the coordination of the dipeptide takes place through the histidine residue and involves the imidazole ring, the amino group, and the amide oxygen.

The infrared data for the dipeptides and the complexes are provided in Tables S-8 and S-9 (Supporting Information), respectively. The amide I and II bands provide clear indications about the coordination mode of the amide group. The amide I band,[65] which largely consists of C═O stretching, is observed at lower energy in the complexes (1632−1642 cm^{-1}) compared with the free ligands (1660−1682 cm^{-1}), in agreement with the reduction of bond order. However, a shift to lower energy could also take place upon deprotonation of the amide nitrogen. For instance, Stocco and co-workers[66] found this band in the 1604−1641 cm^{-1} region for diorganotin(IV) complexes with His-Gly and other dipeptides, in which the ligand is tridentate N,N,O-coordinated (NH_2, deprotonated amide nitrogen, carboxylate). However, in the latter case, the amide II band (out-of-phase combination of N−H deformation and C−N stretching) disappeared. For our complexes, the amide II band is observed at ∼1565 cm^{-1}, virtually unmoved with respect to the free dipeptides. The presence of both vibrations for all compounds is consistent with the coordination of the oxygen of a nondeprotonated amide group in all cases. On the other hand, the fact that the carboxylic group is nondeprotonated and uncoordinated is evidenced from the characteristic bands for this group at their normal positions (cm^{-1}): 1725−1741, ν(C═O); ∼1385, δ(OH); ∼1195, ν(C−O); ∼922, δ(OH).[67]

The strong ν(Re═O) band is observed in the 1000−1015 cm^{-1} range. This high frequency is indicative of a high bond order and consistent with the low donor strength of the *trans* C═O group. This vibration was also observed at high frequencies for the *trans* donors triphenylphosphine oxide (1000 cm^{-1} in $[ReOCl_2(OPPh_3)(2,2'\text{-biimidazole})]Cl$)[68] or carboxylate (1008 cm^{-1} in $ReOX_2$(his)[13] and 993 cm^{-1} in $ReOX_2$(met) (vide infra)). As a comparison, in *mer*- and *fac*-$ReOCl_3$(*N*,*N*′-dimethylbiimidazole),[68] the ν(Re═O) modes occurred at 985 (*trans* imidazole nitrogen) and 970 cm^{-1} (*trans* Cl). The band expected at ∼912 cm^{-1} for the $[ReO_4]^-$ counterion[69] present in the chloro compounds was not identified, since moderately strong bands appear for all ligands in this region.

Crystal Structure of 5a. The asymmetric unit contains two independent, but very similar, $[ReOBr_2(His\text{-}Ala)]^+$ complex cations. The dipeptide is coordinated through the histidine residue, and it acts as a tridentate ligand via an imidazole nitrogen, the NH_2 group, and the carbonyl oxygen of the peptide bond (Figure 4). The alanine residue does not participate in the coordination, and its terminal carboxylic group retains its proton. Thus, this cation includes an

(65) Dollish, F. R.; Fateley, W. G.; Bentley, F. F. *Characteristic Raman Frequencies of Organic Compounds*; Wiley Interscience: New York, 1974; pp 127−133.
(66) Guli, G.; Gennaro, G.; Pellerito, L.; Stocco, G. C. *Appl. Organomet. Chem.* **1993**, *7*, 407−412.
(67) Wolfs, I.; Desseyn, H. O. *Appl. Spectrosc.* **1996**, *50*, 1000−1006.
(68) Fortin, S.; Beauchamp, A. L. *Inorg. Chem.* **2000**, *39*, 4886−4893.
(69) Nakamoto, K. *Infrared and Raman Spectra of Inorganic and Coordination Compounds*; J. Wiley: New York, 1997.

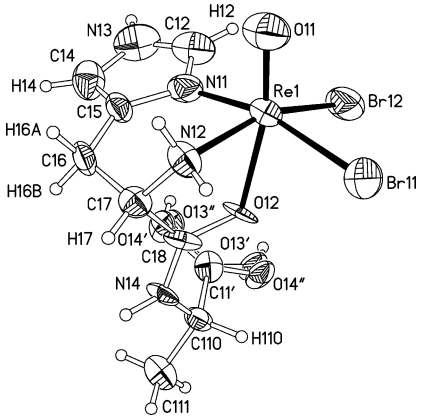

Figure 4. ORTEP drawing of one of the two independent molecules in the asymmetric unit of [$ReOBr_2$(His-Ala)]Br·1/2H_2O·2CH_3CN (**5a**). The other molecule has a very similar structure. In the numbering scheme, the first digit corresponds to the number of the molecule, and the second digit indicates the position. The lattice H_2O and CH_3CN molecules are not shown. Ellipsoids correspond to 40% probability.

equatorial *cis*-N_2Br_2 arrangement like $ReOX_2$(his),[13] whereas the amide oxygen lies *trans* to the Re═O bond, the position occupied by a carboxylato oxygen in the histidine complex. Cysteine, penicillamine, and methionine adopt a similar binding pattern, the S-donor occupying the site filled here by the imidazole unit.[52−54,70,71]

Amide oxygen coordination to rhenium is not common, but examples are known with ligands also containing a phosphine or a sulfur donor,[72−75] and with peptide-like ligand analogues of mercaptoacetyltriglycine.[76] In the present case, considering that the two N donor groups are the same as in the $ReOX_2$(his) complexes[13] and that the *syn*-H_7 conformation positioning the carboxylate group opposite to the Re═O bond was the only one observed, it is not surprising that the same overall arrangement of donors be retained for the peptide complex. This further agrees with the well documented trend for an oxygen to occupy the site *trans* to the Re═O bond.

Selected bond lengths are listed in Table 6. The Re═O distance (mean 1.66 Å) is normal, but the Re−O bond (mean 2.168 Å) is much longer than those of the $ReOX_2$(his)[13] and $ReOX_2$(met) complexes (2.07 Å), which reflects the lower donor ability of the amide oxygen. As noted previously,[13] the Re−N(Im) distances (mean 2.10 Å) are ∼0.05 Å shorter than the Re−NH_2 bonds (2.15 Å), whereas the Re−Br1 bond (trans to Im, 2.492 Å) is longer than the Re−Br2 bond (trans to NH_2, 2.467 Å). The C8−O2 distance (mean 1.26 Å) seems to have increased in the complex, whereas the C8−N4 distance (mean 1.29 Å) has decreased compared to that of the free dipeptides (1.230, $\sigma = 0.008$ Å and 1.328, $\sigma = 0.008$ Å, 11 data). This is consistent with a reduced C═O and an increased C8−N4 bond order after coordination.

Table 6. Selected Bond Lengths in Compound **5a**

	molecule 1	molecule 2	lit.[a]
Re═O	1.654(8)	1.676(8)	1.67(2)[b]
Re−O	2.160(6)	2.176(6)	2.07(2)[b]
Re−NH_2	2.157(7)	2.150(7)	2.15(2)[b]
Re−N(Im)	2.08(1)	2.11(1)	2.10(1)[b]
Re−Br1	2.490(2)	2.495(2)	2.53(4)[b]
Re−Br2	2.468(1)	2.466(2)	2.49(2)[b]
C8−O2	1.27(1)	1.25(1)	1.23(1)[c]
C−O	1.306[d]	1.306[d]	1.30(1)[b]
C═O	1.207[d]	1.207[d]	1.21(1)[b]
C8−N4	1.28(1)	1.30(1)	1.33(1)[c]
C10−N4	1.45(1)	1.45(1)	1.45(1)[c]
C6−C7	1.49(1)	1.51(1)	1.54(1)[c]
C7−C8	1.50(1)	1.48(1)	1.53(1)[c]

[a] Mean values (standard deviations, number of data between 4 and 12). [b] In the structures of $ReOX_2$(his),[13] {$OReBr_2$(hisMe)}$_2O$,[13] and $ReOX_2$(met) (see above). [c] In free His-aa dipeptides (11 data). [d] Distances fixed during the refinement of the disordered carboxylic group.

The octahedron shows a large departure from ideality, mainly due to the Re atom being displaced by 0.36 Å from the N_2Br_2 plane on the oxo side. This distortion is greater than that found in the histidine and methionine complexes (0.32 and 0.28 Å, respectively), probably because the amide C═O group is a weaker donor. As a result, the O═Re−L_{cis} angles (95−106°, Table S-10, Supporting Information) are substantially greater than 90°, whereas similar deviations in the other direction are found on the O−Re−L_{cis} angles (72−87°). Amide oxygen coordination takes place with a normal C8−O2−Re angle of ∼117°. A detailed description of the geometry of the coordinated dipeptide is available in the Supporting Information (Table S-11).

The two crystallographically independent cationic complexes in the asymmetric unit are connected into a dimeric unit by means of two complementary O−H···O hydrogen bonds between the carboxylic acid ends of the dipeptides (Figure S-4 and Table S-12, Supporting Information).

^{1}H NMR Spectroscopy of the Dipeptide Complexes. The NMR data for the dipeptides and the rhenium complexes in CD_3OD are collected in Table 7. All spectra contained second-order signals, whose chemical shifts and coupling constants were determined with the NUTS software.[57] Most of the resonances were readily assigned by comparison with the $ReOX_2$(his) complexes[13] and free peptides. The signals of the inequivalent H_6 protons were assigned individually on the basis of multiplicity. As shown in Figure 5, both signals showed couplings with H_7 (3−4 Hz) and the other H_6 proton (17−18 Hz), but the lower-field signal appeared as a clear doublet of doublets of doublets, whose extra splitting is due a long-range ^4J coupling of 1.7 Hz with the imidazole H_4 proton. A similar $^4J(CH_3-H_5)$ allyl coupling of 2 Hz was observed in 4-methylthiazole.[77] This type of coupling is maximized when the angle between the C−H bond and the plane of the multiple bond (imidazole ring) is 90°. In the above crystal structure, the torsion angles are ca. −78° for $H_{6A}-C_6-C_5-C_4$ and 39° for $H_{6B}-C_6-C_5-C_4$.

(70) Kirsch, S.; Noll, B.; Scheller, D.; Klostermann, K.; Leibnitz, P.; Spies, H.; Johannsen, B. *Forschungszent. Rossendorf* **1996**, *FZR-122*, 110−114.
(71) Kirsch, S.; Noll, B.; Spies, H.; Leibnitz, P.; Scheller, D.; Johannsen, B. *Forschungszent. Rossendorf [Ber.] FZR* **1997**, *FZR-165*, 50−55.
(72) Noll, B.; Noll, S.; Leibnitz, P.; Spies, H.; Schultze, P. E.; Semmler, W.; Johannsen, B. *Inorg. Chim. Acta* **1997**, *255*, 399−403.
(73) Correia, J. D. G.; Domingos, A.; Santos, I. *Eur. J. Inorg. Chem.* **2000**, 1523−1529.
(74) Correia, J. D. G.; Domingos, A.; Paulo, A.; Santos, I. *J. Chem. Soc., Dalton Trans.* **2000**, 2477−2482.
(75) Correia, J. D. G.; Domingos, A.; Santos, I.; Alberto, R.; Ortner, K. *Inorg. Chem.* **2001**, *40*, 5147−5151.
(76) Lipowska, M.; Hansen, L.; Xu, X. L.; Marzilli, P. A.; Taylor, A.; Marzilli, L. G. *Inorg. Chem.* **2002**, *41*, 3032−3041.
(77) Taurins, A.; Schneider, G. *Can. J. Chem.* **1960**, *38*, 1237−1239.

Table 7. ^{1}H NMR Chemical Shifts (ppm) and Coupling Constants (in Brackets, Hz) for the Free Dipeptides and the Rhenium Complexes[a]

	H_2	H_4	H_{6A}	H_{6B}	H_7	H_{10}	H_R
His-Ala	7.885s	7.057s	3.230; 3.194m		4.034t	4.259q	1.415d ($-CH_3$)
			[5.6; 5.8; 15.0]		[5.6; 5.8]	[7.2]	[7.3]
4 (Cl)	8.879s	7.424s	3.843ddd	3.767dd	5.072t	4.128q	1.336d
			[3.0; 17.6; 1.7]	[4.3; 17.6]	[3.0; 4.3]	[7.1]	[7.3]
5 (Br)	9.095s	7.425s	3.891ddd	3.814dd	5.025t	4.094q	1.327d
			[3.3; 17.7; 1.7]	[4.1; 17.7]	[3.3; 4.1]	[7.4]	[7.3]
His-Gly	7.784s	7.010s	3.155; 3.125m		3.991t	3.796; 3.756 ($-CH_2$)	
			[6.1; 6.4; 15.1]		[6.1; 6.4]	[17.0]	
6 (Cl)	8.892s	7.435s	3.845ddd	3.768dd	5.109t	3.826; 3.802	
			[3.1; 17.5; 1.7]	[4.3; 17.5]	[3.1; 4.3]	[17.7]	
7 (Br)	9.107s	7.442s	3.895ddd	3.821dd	5.059t	3.807; 3.787	
			[3.3; 17.5; 1.8]	[4.1; 17.5]	[3.3; 4.1]	[17.8]	
His-Leu	7.774s	6.988s	3.208; 3.155m		3.947t	4.238dd	0.963d; 0.938d ($-CH_3$)
			[5.6; 5.3; 15.0]		[5.6; 5.3]	[3.8; 10.5]	[6.2; 6.0]
							1.60−1.75m ($-CH_2$; $-CH$)
10 (Cl)	8.879s	7.419s	3.852ddd	3.776dd	5.066t	4.090dd	0.911d; 0.836d
			[3.3; 17.6; 2.0]	[4.3; 17.6]	[3.3; 4.3]	[2.4; 12.3]	[6.2; 6.2]
							1.50−1.58m
11 (Br)	9.091s	7.429s	3.903ddd	3.822dd	5.018t	4.060dd	0.901d; 0.819d
			[3.3; 17.7; 1.8]	[4.2; 17.7]	[3.3; 4.2]	[1.6; 13.1]	[6.3; 6.2]
							1.50−1.58m
His-Phe	7.762s	6.969s	3.185; 3.133m		3.901t	4.544dd	2.947dd; 3.166dd ($-CH_2$)
			[5.2; 6.2; 15.0]		[5.2; 6.2]	[4.1; 9.6]	[4.1; 9.6; 14.0]
							7.257m (Ph)
8 (Cl)	8.884s	7.400s	3.814ddd	3.745dd	4.983t	4.413dd	2.932dd; 3.134dd
			[3.1; 17.6; 1.8]	[4.1; 17.6]	[3.1; 4.1]	[4.9; 8.6]	[4.9; 8.7; 14.5]
							7.13−7.31m
9 (Br)	9.102s	7.406s	3.856ddd	3.771dd	4.907dd	4.391dd	2.930dd; 3.118dd
			[3.5; 17.7; 1.8]	[4.0; 17.7]	[3.5; 4.0]	[5.0;8.5]	[4.8; 8.5; 14.6]
							7.11−7.31m

[a] In CD_3OD.

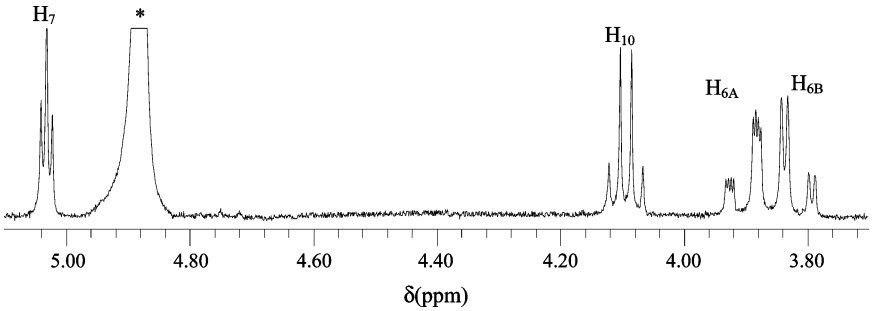

Figure 5. Region of the aliphatic protons in the ^{1}H NMR spectrum of [$ReOBr_2$(His-Ala)]Br (**5**) in CD_3OD. Asterisk indicates water signal.

Accordingly, the low-field signal at ∼3.87 ppm is assigned to H_{6A}. This assignment is further supported by the fact that H_{6A} appears downfield from H_{6B}: protons lying on the *endo* face (Re═O side) of the octahedron like H_{6A} (Figure 4) are generally more deshielded than those on the *exo* side like H_{6B}, because of the anisotropy effects of the Re═O bond.[78−81] By introducing the ^3J coupling constants of 3.3 and 4.1 Hz (estimated accuracy of ±0.5 Hz) into the MULDER program,[58] the H_{6A}—C_6—C_7—H_7 and H_{6B}—C_6—C_7—H_7 torsion angles were calculated to be 64° (±4°) and −56° (±4°), respectively, in good agreement with the values of ∼62° and ∼ −55° observed in the crystal structure of **5a**.

Table 8. Averaged ^{1}H Chemical Shifts (ppm) for the Histidine Residue in N-Terminal Histidine Dipeptides and Their Rhenium Complexes

	H_2	H_4	H_{6A}	H_{6B}	$\Delta\delta_{6A/6B}$	H_7
His-X[a] (DMSO)			3.10	3.06	0.04	4.05
His-aa (CD_3OD)	7.80	7.01	3.19	3.15	0.04	3.97
[$ReOCl_2$(His-aa)]Cl	8.88	7.42	3.84	3.76	0.08	5.06
[$ReOBr_2$(His-aa)]Br	9.10	7.43	3.89	3.81	0.08	5.00

[a] X = Ala, Gly, Leu, Ser, Lys, Phe, Tyr. From ref 82.

The chemical shifts of H_2, H_4, $H_{6A/6B}$, and H_7 in the histidine unit are not very sensitive to the other residue present in the dipeptide. These signals shift upon complexation, but the variation from one complex to another is small, thereby showing that the coordination mode remains the same for the various peptides. The average values are listed in Table 8 and compared with the results reported for the free dipeptides. As noted with the histidine complexes, coordination induces downfield shifts on all histidine protons. The deshielding is more pronounced (∼1 ppm) for H_2 and H_7 than for H_4 and $H_{6A/6B}$ (0.4 and 0.7 ppm, respectively), in agreement with the respective distances of these protons from the coordination center.

(78) Hansen, L.; Xu, X. L.; Lipowska, M.; Taylor, A.; Marzilli, L. G. *Inorg. Chem.* **1999**, *38*, 2890−2897.
(79) Oneil, J. P.; Wilson, S. R.; Katzenellenbogen, J. A. *Inorg. Chem.* **1994**, *33*, 319−323.
(80) Papadopoulos, M. S.; Pirmettis, I. C.; Pelecanou, M.; Raptopoulou, C. P.; Terzis, A.; Stassinopoulou, C. I.; Chiotellis, E. *Inorg. Chem.* **1996**, *35*, 7377−7383.
(81) Papadopoulos, M. S.; Pelecanou, M.; Pirmettis, I. C.; Spyriounis, D. M.; Raptopoulou, C. P.; Terzis, A.; Stassinopoulou, C. I.; Chiotellis, E. *Inorg. Chem.* **1996**, *35*, 4478−4483.

Table 9. Averaged Coupling Constants (Hz) for the Histidine Residue in N-Terminal Histidine Dipeptides and Their Rhenium Complexes

	$^3J(H_{6A}-H_7)$	$^3J(H_{6B}-H_7)$	$^3J(H_{6A}-H_{6B})$	$^4J(H_4-H_{6A})$
His-aa (CD_3OD)	5.6	5.9	15.0	0
$[ReOCl_2$-(His-aa)]Cl	3.1	4.3	17.6	1.8
$[ReOBr_2$-(His-aa)]Br	3.4	4.1	17.7	1.8

Scheme 4

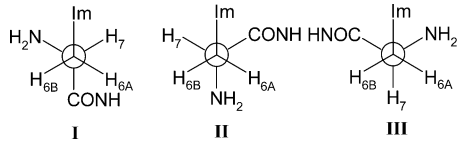

The chemical shift difference $\Delta\delta_{6A/6B}$ (anisochrony)[82] increases appreciably in the complexes (0.08 ppm, Table 8) compared with the free ligands (0.04 ppm). A possible contribution to this effect is the anisotropy of the Re═O bond mentioned above, which produces a deshielding of the proton occupying the same side of the molecule. On the other hand, Fermandjian and co-workers have observed a relationship between the anisochrony value and the predominance of a single rotamer in the histidine side chain of the dipeptide.[82] From the values of J_t (12.5 Hz) and J_g (3.25 Hz) used by these authors and the standard equations,[13] our data for the His-aa peptides in CD_3OD (Table 9) led to rotamer populations of 0.25 (**I** or **II**), 0.29 (**II** or **I**), and 0.46 (**III**) (Scheme 4). This roughly uniform distribution of rotamers is consistent with the relatively small anisochrony of 0.04 ppm. In the complexes, conformation **III** is imposed by the facial tridentate coordination and this is well reflected by the coupling constants, since a population of 0.90 is predicted for **III** from the coupling constants of the complexes. The clear predominance of **III** agrees with the greater anisochrony of 0.08 ppm.

For H_{10} and the nearby protons in the side-chains of the C-terminal amino acid, upfield shifts are observed upon coordination (Table 7), except for His-Gly, where these signals are virtually unmoved. Small shielding was also noted for protons of an uncoordinated residue similarly positioned with respect to the $Re{=}O^{3+}$ core in a complex with dimethylglycyl-L-seryl-L-cysteinylglycinamide.[83] This shielding could be related to the anisotropy effects of the Re═O bond, since this part of the dipeptides is located on the *exo* side of the complex. As to the side chain in the C-terminal unit of His-Phe and His-Leu, the ^3J coupling constants between H_{10} and the methylene protons suggest that the conformation about the C_{10}—C_{11} bond is little affected, since the pattern consisting of one small and one large coupling constant, indicative of a *trans* H_{10}—C_{10}—C_{11}—$H_{11(trans)}$ interaction, observed for the free peptides is retained in the complexes.

Concluding Remarks

The S,N,O-coordinated $ReOX_2$(met) complexes reported in the present study are structurally similar to the histidine analogues $ReOX_2$(his) described earlier,[13] the imidazole of histidine being replaced by an SCH_3 group in methionine. However, the presence of the prochiral $S-CH_3$ group generates two diastereoiomers in solution, so that the product can be regarded as a mixture of two components each with its own characteristics. Furthermore, preliminary results indicate that the $Re-SCH_3$ bond is relatively labile, and this, probably combined with a reduced stabilization of the six-membered Re−N−C−C−C−S chelate (compared with the five-membered Re−N−C−C−N ring of histidine), makes the present methionine complexes much more receptive to ring opening and ligand substitution. For instance, traces of water seem to initiate a cascade of processes leading to complete deligation of methionine. These peculiarities make methionine less attractive than histidine as a component of a BFCA to carry hot Tc or Re nuclei. Therefore, our efforts were redirected toward histidine as terminal residue and dipeptides containing N-terminal histidine were examined.

The four dipeptides studied react with $ReOX_3(OPPh_3)(Me_2S)$ following the same pattern as histidine itself, leading to species in which a *facial* $O{=}ReX_2$ core is retained. Coordination is largely controlled by strong binding of the terminal NH_2 group and the available imidazole nitrogen in the equatorial plane perpendicular to the Re═O bond. Once these donors are coordinated, the ligand adopts a conformation that positions the amide oxygen at the sixth coordination site, *trans* to the Re═O bond. The marked preference for the oxo−rhenium molecules to accept an oxygen ligand *trans* to the Re═O bond seems to balance the fact that this oxygen is not ideally positioned (O═Re—O angle of 166°) and that the bond is rather weak. The replacement of an already weak Re—O(carboxylate) bond of the histidine compounds by a still weaker Re—O(amide) bond with the dipeptides does change the overall binding pattern. Since the C-terminal residue does not interfere or contribute in the overall process and does not participate in particular intramolecular nonbonded interactions, it is likely that longer peptide chains would behave similarly and that a $O{=}ReX_2$ core could also be attached to a larger peptide bearing a N-terminal histidine residue.

Acknowledgment. The financial support of the Natural Sciences and Engineering Research Council of Canada is gratefully acknowledged.

Supporting Information Available: X-ray crystallographic files in CIF format for the five structures. Additional details, tables, and figures. This material is available free of charge via the Internet at http://pubs.acs.org.

IC048776E

(82) Haertle, T.; Linter, K.; Piriou, F.; Fermandjian, S. *Int. J. Biol. Macromol.* **1982**, *4*, 335−340.
(83) Wong, E.; Fauconnier, T.; Bennett, S.; Valliant, J.; Nguyen, T.; Lau, F.; Lu, L. F. L.; Pollak, A.; Bell, R. A.; Thornback, J. R. *Inorg. Chem.* **1997**, *36*, 5799−5808.
(84) Flack, H. D. *Acta Crystallogr.* **1983**, *A39*, 876−881.